In the case of a perfect gas ($\gamma =$ constant) with a single progress variable, we can use $h(T)$ (Eq. 3) to specify P in terms of reference quantities.

$$
\begin{aligned}
a'P^2 + b'P + c' = 0 \\
a' &= -\frac{\gamma+1}{2\gamma(\rho \mathrm{u})_r^2} \\
b' &= \frac{1}{\gamma}\left[\frac{P+\rho \mathrm{u}^2}{(\rho \mathrm{u})^2}\right]_r \\
c' &= \frac{1}{2\gamma}\left[\left(\frac{P}{\rho}\right)_r\left[(\gamma-1)\left(\frac{P}{\rho \mathrm{u}^2}\right)_r - 2\right] - \lambda q\frac{\gamma-1}{\gamma}\right]
\end{aligned}
\tag{65}
$$

4.2.2 Differential System

To find the purely differential system of equations, we use the steady form of the one-dimensional reactive Euler equations in the wave-fixed frame (Eq. 55).

$$\mathrm{w}\frac{\mathrm{d}\rho}{\mathrm{d}x} + \rho\frac{\mathrm{dw}}{\mathrm{d}x} = 0 \tag{66}$$

$$\rho \mathrm{w}\frac{\mathrm{dw}}{\mathrm{d}x} + \frac{\mathrm{d}P}{\mathrm{d}x} = 0 \tag{67}$$

$$\mathrm{w}\left(\frac{\mathrm{d}P}{\mathrm{d}x} - \frac{\mathrm{d}\rho}{\mathrm{d}x}\right) = \rho a_f^2\dot{\sigma} \tag{68}$$

$$\mathrm{w}\frac{\mathrm{d}Y_i}{\mathrm{d}x} = \dot{\Omega}_i \tag{69}$$

Equations 66-69 can also be expressed in terms of the sonic parameter,

$$\eta = 1 - M^2, \tag{70}$$

as

$$\frac{\mathrm{d}\rho}{\mathrm{d}x} = -\frac{\rho}{\mathrm{w}}\frac{\dot{\sigma}}{\eta} \tag{71}$$

$$\frac{\mathrm{dw}}{\mathrm{d}x} = \frac{\dot{\sigma}}{\eta} \tag{72}$$

$$\frac{\mathrm{d}P}{\mathrm{d}x} = -\rho \mathrm{w}\frac{\dot{\sigma}}{\eta} \tag{73}$$

$$\mathrm{w}\frac{\mathrm{d}Y_i}{\mathrm{d}x} = \dot{\Omega}_i. \tag{74}$$

In the Lagrangian description, these equations are

$$
\begin{aligned}
\left.\frac{\mathrm{d}\rho}{\mathrm{d}t}\right|_{X_p} &= -\rho\frac{\dot{\sigma}}{\eta} \\
\left.\frac{\mathrm{dw}}{\mathrm{d}t}\right|_{X_p} &= \mathrm{w}\frac{\dot{\sigma}}{\eta} \\
\left.\frac{\mathrm{d}P}{\mathrm{d}t}\right|_{X_p} &= -\rho \mathrm{w}^2\frac{\dot{\sigma}}{\eta} \\
\left.\frac{\mathrm{d}Y_i}{\mathrm{d}t}\right|_{X_p} &= \dot{\Omega}_i.
\end{aligned}
\tag{75}
$$

For either differential system of equations (Eqs. 71-74 or Eq. 75), we can use,

$$\frac{\mathrm{d}t}{\mathrm{d}X_p} = \frac{1}{\mathrm{w}} \quad \text{or} \quad \frac{\mathrm{d}X_p}{\mathrm{d}t} = \mathrm{w} \tag{76}$$

to find the particle path.

It is also interesting to derive an expression for the temperature evolution. To do this, we start with the ideal gas P-v-T equation.

$$P = \rho R T \tag{77}$$

We find the temperature derivative by taking the logarithmic derivative of this equation

$$\frac{\mathrm{d}P}{P} = \frac{\mathrm{d}\rho}{\rho} + \frac{\mathrm{d}R}{R} + \frac{\mathrm{d}T}{T} \tag{78}$$

The definition of the gas-specific gas constant,

$$R = \frac{\mathcal{R}}{\overline{W}} = \mathcal{R} \sum_{i=1}^{N_Y} Y_i / W_i, \tag{79}$$

its derivative,

$$\frac{\mathrm{d}R}{R} = \sum_{i=1}^{N_Y} \frac{\overline{W}}{W_i} \mathrm{d}Y_i, \tag{80}$$

and the ZND equations (Eqs. 71-74) lead to

$$\frac{\mathrm{d}T}{\mathrm{d}x} = \frac{T}{\mathrm{w}} \left[(1 - \gamma M^2) \frac{\dot{\sigma}}{\eta} - \sum_{i=1}^{N_Y} \frac{\overline{W}}{W_i} \dot{\Omega}_i \right] \tag{81}$$

or

$$\left. \frac{\mathrm{d}T}{\mathrm{d}t} \right|_{X_p} = T \left[(1 - \gamma M^2) \frac{\dot{\sigma}}{\eta} - \sum_{i=1}^{N_Y} \frac{\overline{W}}{W_i} \dot{\Omega}_i \right] \tag{82}$$

In these expressions $\mathcal{R}$ is the universal gas constant, $\overline{W}$ is the average molecular weight, and W_i is the weight of species i.

4.2.3 Length Scales

In the ZND detonation model, there are two main length scales: the induction length Δ_i and the energy pulse width Δ_e. We determine these scales from the thermicity profile. Figure 5 indicates that Δ_i is the distance to the maximum thermicity and Δ_e is the half-height width of the thermicity pulse.

4.2.4 Particle Paths

The particle paths shown in Fig. 4 were computed based on the ZND structure of a CJ detonation in stoichiometric hydrogen-air initially at 300 K and 1 bar. In the wave-fixed frame (Fig. 4c), the equations

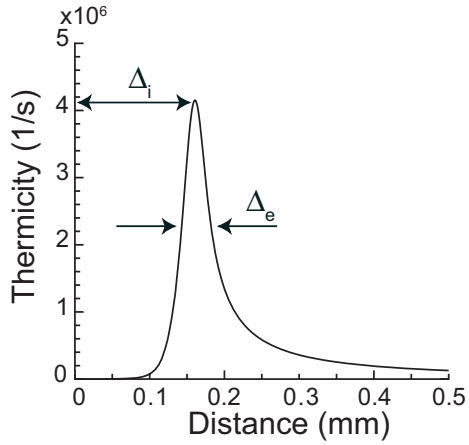

Figure 5: Definition of the induction length Δ_i and energy pulse width Δ_e in terms of the thermicity for a CJ detonation in stoichiometric hydrogen-air initially at 300 K and 1 atm. In this case $\Delta_i = 161$ μm and $\Delta_e = 43$ μm .

are

$$x_S = 0 \tag{83}$$

$$x_{\Delta_i} = \Delta_i \tag{84}$$

$$x_{\pm\Delta_e/2} = \Delta_i \pm \frac{\Delta_e}{2} \tag{85}$$

$$x_M = \Delta_M \tag{86}$$

$$X_p = \int_{t_S}^{t} \mathrm{w}\mathrm{d}t \tag{87}$$

where x_S is the location of the shock (black line), x_{Δ_i} is the end of the induction zone or the location of the thermicity peak (red line), $x_{\pm\Delta_e/2}$ bound the energy release zone (blue lines), x_M is the location of $M = 0.73$ (black dashed line), and X_p is the particle path (green curve). For Figs. 4a and b, we must transform to the lab frame. In these figures, the equations for the lines become

$$x_S^L = \mathrm{U}_S\, t \tag{88}$$

$$x_{\Delta_i}^L = \mathrm{U}_S\, t - \Delta_i \tag{89}$$

$$x_{\pm\Delta_e/2}^L = \mathrm{U}_S\, t - \left(\Delta_i \pm \frac{\Delta_e}{2}\right) \tag{90}$$

$$x_M^L = \mathrm{U}_S\, t - \Delta_M \tag{91}$$

$$X_p^L = \begin{cases} X_p^L(t=0) & t < t_S \\ X_p^L(t=0) + \int_{t_S}^{t} (\mathrm{U} - \mathrm{w})\mathrm{d}t & t \geq t_S \end{cases} \tag{92}$$

where t_S is the time when the shock reaches a particle that was originally at $X_P(t=0)$.

Special care must be taken when generating these curves from the discrete data returned from our implementation. The curves in the wave-fixed frame come directly from the discrete data. The distance column corresponds to $X_p = \int \mathrm{w}\mathrm{d}t$. On the other hand, in the lab frame, creating the discrete particle path array is slightly more challenging. Our implementation uses a variable step size integrator, and

therefore the integrator takes smaller steps within the reaction zone than close to equilibrium. The time array that is returned represents that time elapsed since the shock and particle path intersect. For this reason, "t" in the lab frame particle path equation corresponds to t_S plus the time array starting with the first element to assure that the step size remains the same through the reaction zone for all particle paths.

4.3 Eigenvalue Detonation

If η actually vanishes before $\dot{\sigma}$ does, then the solutions for P and ρ will develop singularities and will have to be discarded as nonphysical. This is how the weak solution branch of the detonation adiabat (see Browne et al., 2007) can be ruled out. In order to reach a weak solution, which is supersonic $\eta < 0$, from a subsonic post-shock state, η will have to pass through zero. Unless $\dot{\sigma}$ vanishes exactly at the point $\eta = 0$, no acceptable solution to the structure equations will exist. This implies that $\dot{\sigma}$ must change sign within the reaction zone exactly at the point where η vanishes. This is termed an *eigenvalue* or *pathological* detonation (Fickett and Davis, 1979).

Physically, eigenvalue solutions can occur if competing exothermic and endothermic reactions (Zel'dovich, 1940) or a decrement in the mole number ($\Delta n < 0$) (von Neumann, 1942) cause $\dot{\sigma}$ to change sign within the reaction zone. Computations described subsequently indicate that realistic reaction mechanisms do tend to predict a weak eigenvalue effect in most fuel-oxidizer systems but it is not clear that this can be experimentally observed. Supersonic states are observed (Edwards et al. ; ?; Duff et al. 1958) behind propagating detonations, but this is related to the presence of the instability waves on the detonation front and boundary layers in ducts rather than eigenvalue-type solutions. The variation from the computed CJ velocity is small and there are a number of complicating factors in interpreting the experiments in terms of idealized one-dimensional models based on reaction mechanisms and thermochemical data that have appreciate uncertainties.

Eigenvalue-type solutions are plausible and have been studied in the context of curved detonation waves and frictional flows. Curvature and gradients in the flow behind the detonation wave can compete with the energy release as discussed in the previous section on the shock change equation. Critical wave speeds and curvatures result from an eigenvalue analysis. If the flow is considered quasi-one dimensional, friction at the walls of the duct will compete with the reaction to produce an eigenvalue situation. Models of detonation failure in narrow channels or ducts have been developed around this idea. REFERENCES

What happens at the end of the reaction zone, $x \to \infty$? For a CJ detonation, the solution of the structure equations should approach the CJ state as $x \to \infty$. As long as $\dot{\sigma}$ approaches zero faster than η does, the solutions will be well behaved and nonsingular. In practice, there is usually no difficulty because the Mach number used to define η is based on the frozen sound speed a_f and the fluid velocity at the end of a CJ reaction zone approaches the equilibrium sound speed, a_e. The value of the frozen sound speed is always between 1 and 10% larger than the equilibrium value at the end of the reaction zone (Fickett and Davis, 1979), so that η never reaches zero. For overdriven waves, the flow always terminates at a subsonic velocity on the detonation adiabat so there is no difficulty with that case either.

4.4 Numerical Methods

This algorithm solves the ZND detonation governing equations to determine the evolution of the thermodynamic state and the induction time. Our implementation returns the two length scales of interest (see Section 4.2.3), the induction length Δ_i and the energy pulse width Δ_e. By integrating the particle path (Eq. 76), we also return the corresponding induction time τ_i and energy pulse time τ_i.

4.4.1 Initial Conditions

The initial conditions for the simulation are that of a shocked gas mixture. The user must specify the pre-shock initial conditions and either the desired shock speed or the option to use the Chapman-Jouguet detonation speed for the given mixture.

ADD MACH NUMBER CHECK

4.4.2 Algorithm

1. Define known quantities: Upstream State (P_1, T_1, $\overline{Y}_1$), $\overline{W}$, $\mathcal{R}$, error tolerances
2. Seek unknown quantities: Evolution of thermodynamic properties and species ($P(t)$, $T(t)$, $\overline{Y}(t)$) and Induction Time
3. Call program `PostShock` (Browne et al., 2007) to determine the initial conditions for the ZND detonation simulation
   - The `znd_shk` option implements `PostShock_fr` and requires the user to specify the shock speed.
   - The `znd_CJ` option implements `PostShock_fr` and assumes that the shock speed will be the CJ speed.
4. Call a stiff ODE solver (`ode15s` in Matlab, `CVODE` in c++) to iteratively solve Eqs. 71-74 and Eq. 76 subject to the equation of state (Eq. 2) and the definitions of thermicity (Eqs. 42 and 45) and the sonic parameter (Eq. 70).
5. Create an array of the thermicity according to Eqs. 42 and 45.
6. Find the induction length Δ_i, induction time τ_i, exothermic pulse width Δ_e, and exothermic pulse time τ_e in terms of the thermicity.
7. Return $\Delta_i, \tau_i, \Delta_e, \tau_e$, and arrays for $P(t)$, $T(t)$, and $\overline{Y}(t)$

Figure 6 shows the agreement of our new implementation with the legacy Fortran version which uses the CHEMKIN thermodynamic library.

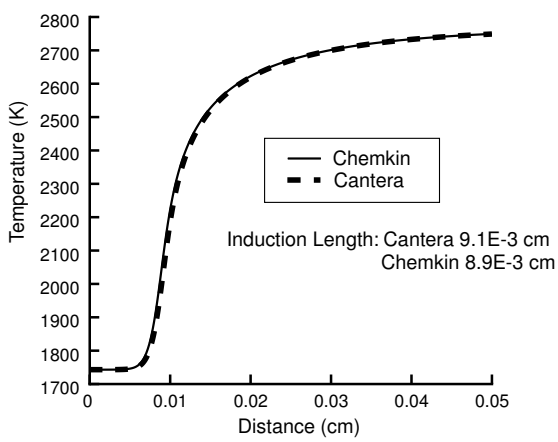

Figure 6: ZND detonation temperature profile simulated by our implementation superimposed over ZND detonation temperature profile simulated by Shepherd's ZND program. The case is hydrogen air with an equivalence ratio of 0.5, an initial temperature of 300 K, an initial pressure of 1 atm, and a shock speed of 2000 m/s.

4.5 Examples

Here will illustrate the results for a CJ detonation and an overdriven detonation. There is no solution for an underdriven detonation (see Browne et al. (2007) for a detailed explanation). See the following examples:
Matlab: demo_ZNDCJ.m and demo_ZNDshk.m
C++: ZND_Basic
Python/C++: znd.py

4.5.1 CJ Detonation

The Chapman-Jouguet detonation velocity is the minimum wave speed that admits a solution. The CJ case is depiced in the P-v plane in Fig. 3. We see that the Rayleigh line is tangent to the product Hugoniot. The spatial profiles for pressure, temperature, density, velocity, and species for a CJ detonation in an initially stoichiometric mixture of hydrogen and air at 300 K and 1 atm is shown in Figs. 7 and 8. We used the Matlab demonstration demo_ZNDCJ.m to generate these results. The thermicity profile for this case is superposed on the temperature profile and shown in Figure 9.

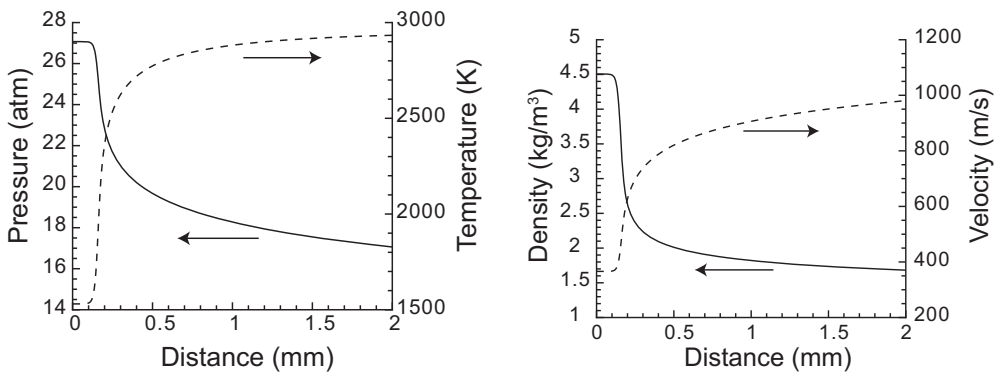

(a) (b)

Figure 7: ZND structure for a CJ detonation stoichiometric hydrogen-air initially at 300 K and 1 atm. (a) temperature and pressure profiles, (b) density and velocity profiles

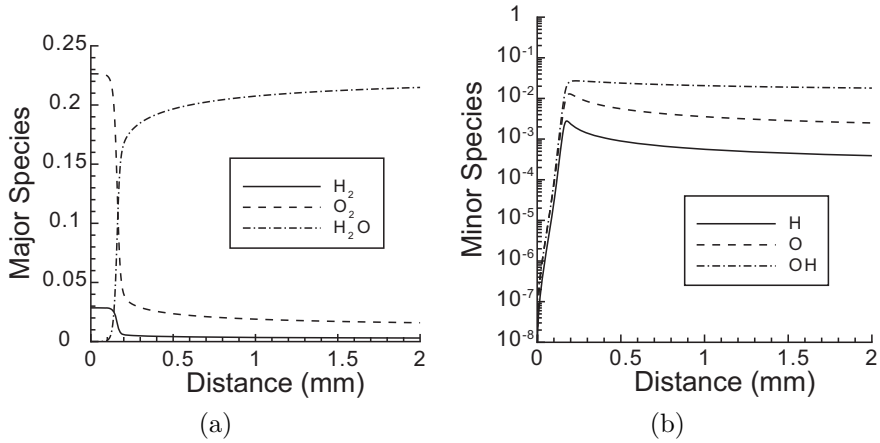

(a) (b)

Figure 8: ZND structure for a CJ detonation stoichiometric hydrogen-air initially at 300 K and 1 atm. (a) major species profiles, (b) minor species profiles

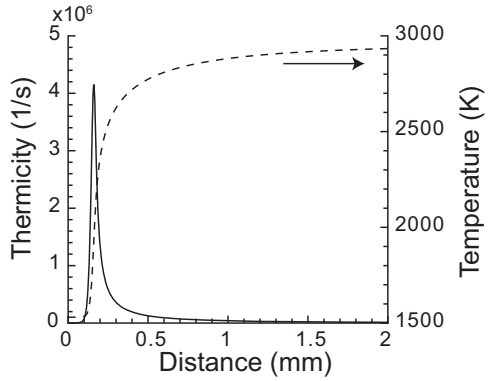

Figure 9: Thermicity ($\dot{\sigma}$) and temperature ZND structure for a CJ detonation in stoichiometric hydrogen-air initially at 300 K and 1 atm.

4.5.2 Overdriven Detonation

If we increase the speed of the front shock, the Rayleigh line becomes steeper. This is shown in Fig. 10 for U = 1.1U$_{CJ}$. Unless we have an eigenvalue detonation (see Section 4.3), only the upper intersection,

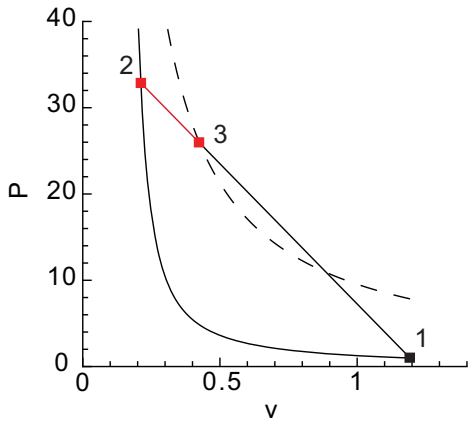

Figure 10: Path (red) between frozen Hugoniot (solid) and equilibrium Hugoniot (dashed) for a ZND detonation traveling at U = 1.1U$_{CJ}$.

the strong solution, is admissible. The spatial profiles for pressure, temperature, density, velocity, and species for an overdriven detonation (U = 1.1U$_{CJ}$) in an initially stoichiometric mixture of hydrogen and air at 300 K and 1 atm is shown in Figs. 7 and 8. We used the Matlab demonstration demo_ZNDshk.m to generate these results. The thermicity profile for this case is superposed on the temperature profile and shown in Fig. 13.

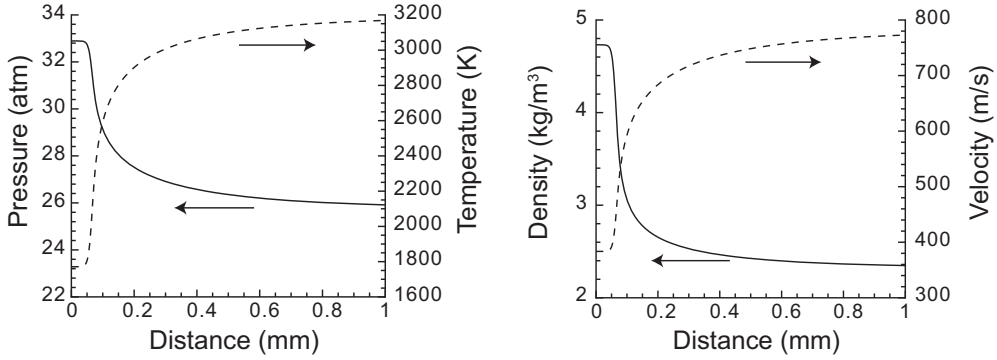

(a) (b)

Figure 11: ZND structure for an overdriven detonation (U = 1.1U$_{CJ}$) stoichiometric hydrogen-air initially at 300 K and 1 atm. (a) temperature and pressure profiles, (b) density and velocity profiles

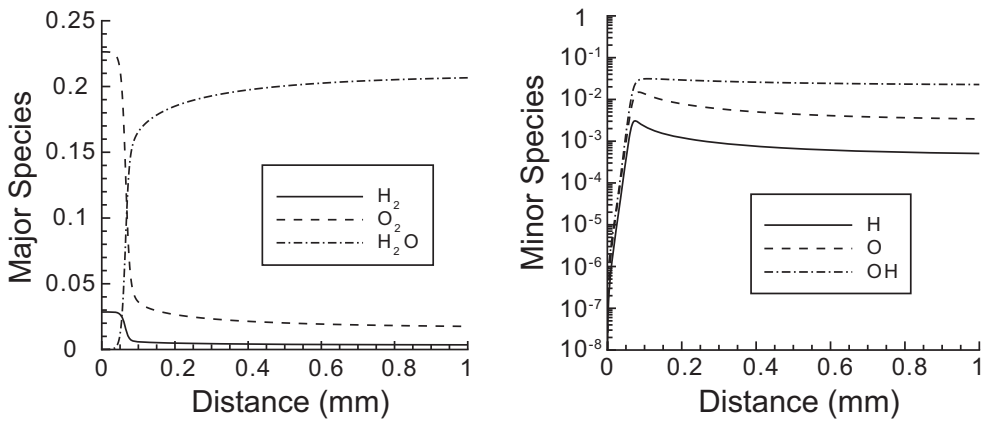

(a) (b)

Figure 12: ZND structure for an overdriven detonation (U = 1.1U$_{CJ}$) stoichiometric hydrogen-air initially at 300 K and 1 atm. (a) major species profiles, (b) minor species profiles

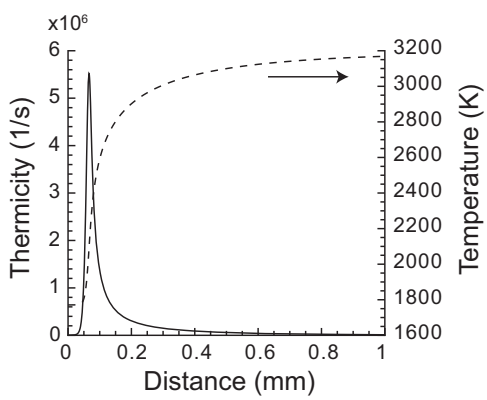

Figure 13: Thermicity ($\dot{\sigma}$) and temperature ZND structure for an overdriven detonation (U = 1.1U$_{CJ}$) stoichiometric hydrogen-air initially at 300 K and 1 atm.

5 Extensions to the ZND model

Three useful extensions to the ZND model equations have been developed. Eckett et al. (2000) derived the model in the case of a unsteady curved front shock. Klein et al. (1995) describes a subset of this unsteady model which focuses specifically on curved waves. CITE MCGILL give a model that includes frictional effects.

5.1 Unsteady Model

Eckett et al. (2000) derives an extension of the ZND model by including geometry and unsteadiness in the leading shock. The reactive Euler equations for the most general case are

$$\begin{aligned}
\frac{\mathrm{D}\rho}{\mathrm{D}t^L} + \rho\frac{\partial \mathrm{u}}{\partial x^L} + \frac{j}{x^L}\rho\mathrm{u} &= 0 \\
\frac{\mathrm{D}\mathrm{u}}{\mathrm{D}t^L} + \frac{1}{\rho}\frac{\partial P}{\partial r^L} &= 0 \\
\frac{\mathrm{D}P}{\mathrm{D}t^L} - a_f^2\frac{\mathrm{D}\rho}{\mathrm{D}t^L} &= \rho a_f^2\dot{\sigma} \\
\frac{\mathrm{D}Y_i}{\mathrm{D}t^L} &= \dot{\Omega}_i
\end{aligned} \tag{93}$$

where j is the dimensionality, i.e. $j = 0$ for a planar shock, $j = 1$ for a cylindrical shock, or $j = 2$ for a spherical shock. If we assume that the shock speed U is only a function of time, these can be rewritten in the wave-fixed frame in terms of $\dot{\sigma}$ and η.

$$\begin{aligned}
\eta\frac{\mathrm{D}\rho}{\mathrm{D}t} &= -\rho\dot{\sigma} + \frac{j}{X_S - x}\rho M^2(\mathrm{U} - \mathrm{w}) + \frac{\rho\mathrm{w}}{a_f^2}\frac{\mathrm{dU}}{\mathrm{d}t} - \frac{\rho\mathrm{w}}{a_f^2}\frac{\partial \mathrm{w}}{\partial t} + \frac{1}{a_f^2}\frac{\partial P}{\partial t} \\
\eta\frac{\mathrm{Dw}}{\mathrm{D}t} &= \mathrm{w}\dot{\sigma} - \frac{j}{X_S - x}\mathrm{w}(\mathrm{U} - \mathrm{w}) - M^2\frac{\mathrm{dU}}{\mathrm{d}t} + \frac{\partial \mathrm{w}}{\partial t} - \frac{\mathrm{w}}{\rho a_f^2}\frac{\partial P}{\partial t} \\
\eta\frac{\mathrm{D}P}{\mathrm{D}t} &= -\rho\mathrm{w}^2\dot{\sigma} + \frac{j}{X_S - x}\rho\mathrm{w}^2(\mathrm{U} - \mathrm{w}) + \rho\mathrm{w}\frac{\mathrm{dU}}{\mathrm{d}t} - \rho\mathrm{w}\frac{\partial \mathrm{w}}{\partial t} + \frac{\partial P}{\partial t} \\
\frac{\mathrm{D}Y_i}{\mathrm{D}t} &= \dot{\Omega}_i
\end{aligned} \tag{94}$$

where X_S is the location of the shock. The rate of change of temperature for this model is

$$\begin{aligned}
\eta c_P\frac{\mathrm{D}T}{\mathrm{D}t} = &-(1 - \gamma M^2)\sum e_i\dot{\Omega}_i - \frac{a_f^2}{\gamma}\sum\frac{\overline{W}}{W_i}\dot{\Omega}_i \\
&+ \frac{j}{X_S - x}\mathrm{w}^2(\mathrm{U} - \mathrm{w}) + \mathrm{w}\frac{\mathrm{dU}}{\mathrm{d}t} - \mathrm{w}\frac{\partial \mathrm{w}}{\partial t} + \frac{1}{\rho}\frac{\partial P}{\partial t}
\end{aligned} \tag{95}$$

If the shock is planar and the detonation is steady, these equations reduce to the ZND equations (Eqs. 71-74) presented in Section 4.

5.2 Steady Curved Wave Model

Klein et al. (1995) present an extension of the ZND model that allows for curvature only of the front wave. The define a normalized stream tube area change (Bdzil and Stewart, 1988)

$$\alpha = \frac{1}{A}\frac{\mathrm{d}A}{\mathrm{d}x} = \frac{j}{X_S}\left(\frac{U}{\mathrm{w}} - 1\right) \tag{96}$$

Again j is the dimensionality and X_S is the location of the shock. In terms of α, the extension of the ZND model is

$$\begin{aligned}
\frac{\mathrm{d}\rho}{\mathrm{d}x} &= -\frac{\rho}{\mathrm{w}}\frac{(\dot{\sigma} - \mathrm{w}M^2\alpha)}{\eta} \\
\frac{\mathrm{dw}}{\mathrm{d}x} &= \frac{(\dot{\sigma} - \mathrm{w}\alpha)}{\eta} \\
\frac{\mathrm{d}P}{\mathrm{d}x} &= -\rho\mathrm{w}\frac{(\dot{\sigma} - \mathrm{w}\alpha)}{\eta} \\
\frac{\mathrm{d}Y_i}{\mathrm{d}x} &= \frac{\dot{\Omega}_i}{\mathrm{w}}
\end{aligned} \tag{97}$$

In the case of a planar shock, these reduce to the ZND equations (Eqs. 71-74) presented in Section 4.

5.3 Steady Detonation with Friction

ADD SECTION

6 Constant Volume Explosion Model

In this section, we will present the constant volume explosion model which is a limiting case of the ZND model (see Section 4). We will first give a graphical interpretation and present the mathematical model. Then we will describe our algorithm, and finally give an example.

6.1 Physical Model

The ZND model (Section 4) involves both chemical reaction and fluid dynamics. A simplier model could monitor a small constant volume packet of reacting gas. As described in Section 3, tracking the time evolution of a fluid packet is the Langragian description of the field. If the specific volume is held constant, the Rayleigh line between the reactant and product Hugoniot curves is vertical as shown in Figure 14 which implies infinitely fast combustion ($\mathrm{w} \to \infty$).

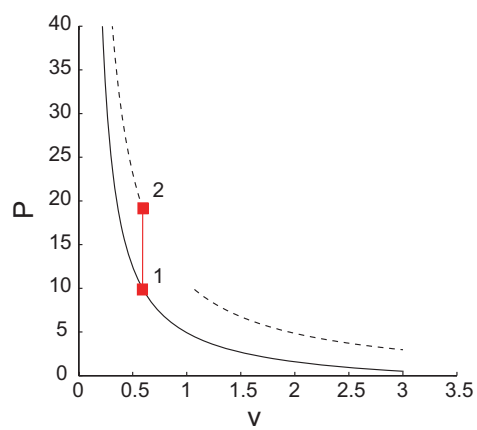

Figure 14: Path (blue) between frozen Hugoniot (solid) and equilibrium Hugoniot (dashed) for a constant volume explosion.

6.2 Mathematical Model

Like the ZND model (Section 4), the constant volume explosion model can be expressed as a differential species conservation equation subject to algebraic physical constraints or as a purely differental system of equations.

6.2.1 Algebraic Differential System

The algebraic-differential system of equations corresponds to the Lagrangian conservation of species equation

$$\left.\frac{\mathrm{d}Y_i}{\mathrm{d}t}\right|_{X_p} = \dot{\Omega}_i, \tag{98}$$

where X_p is the particle path, and an algebraic constraint determined by the shock jump conditions (Eq. 15). The simplest way to specify this algebraic constraint is to examine the following form of the Hugoniot curve equation

$$\Delta e = \Delta v \frac{P_1 + P_2}{2}. \tag{99}$$

We see that if the volume is constant then,

$$\Delta e = 0 \tag{100}$$

which is appropriate because in a rigid isolated system, energy is conserved. In the case of a perfect gas ($\gamma =$ constant) with a single progress variable, we can use

$$e(T) = \frac{1}{\gamma - 1}\frac{P}{\rho} - \lambda q \tag{101}$$

to specify P in terms of species.

$$P = (\gamma - 1)\frac{e(T) + \lambda q}{\rho} \tag{102}$$

6.2.2 Differential System

The constant volume explosion model is a Lagrangian model and therefore appears to be an unsteady zero-dimensional system of equations. For this model, we recall the definition of η (Eq. 70) and look at the limiting behavior of Eq. 75 as the velocity goes to infinity. The limiting equations are

$$\left.\frac{\mathrm{d}\rho}{\mathrm{d}t}\right|_{X_p} = 0 \tag{103}$$

$$\left.\frac{\mathrm{d}\mathrm{w}}{\mathrm{d}t}\right|_{X_p} = 0 \tag{104}$$

$$\left.\frac{\mathrm{d}P}{\mathrm{d}t}\right|_{X_p} = -\rho a_f^2 \dot{\sigma} \tag{105}$$

$$\left.\frac{\mathrm{d}Y_i}{\mathrm{d}t}\right|_{X_p} = \dot{\Omega}_i. \tag{106}$$

We find that as expected the density (or specific volume) remains constant and the pressure varies. We could also use the constant volume limit of Eq. 26.

$$\left.\frac{\mathrm{d}e}{\mathrm{d}t}\right|_{X_p} = 0 \tag{107}$$

This corresponds more directly to Eq. 100. Most commonly, we compute the temperature as a function of time. The temperature equation can be derived from either energy equation (Eq. 105 or Eq. 107) or as the limit of the ZND temperature evolution equation (Eq. 82).

$$\left.\frac{\mathrm{d}T}{\mathrm{d}t}\right|_{X_p} = -\frac{1}{c_v}\sum_{i=1}^{N_Y} e_i \dot{\Omega}_i \tag{108}$$

A more detailed derivation of Eq. 108 is given in Appendix A

6.2.3 Time Scales

In the CV detonation model, there is one main time scale: the induction time τ_i. We determine this scale from the temperature gradient profile. Figure 15 indicates that τ_i is the time to the maximum temperature gradient.

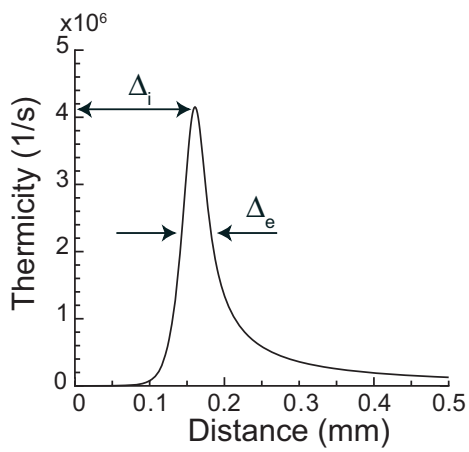

Figure 15: Definition of the induction time τ_i in terms of the temperature gradient for a constant volume explosion in stoichiometric hydrogen-air initially at the von Neumann point. In this case $\tau_i = 161$ μs.

6.3 Numerical Method

The algorithm below solves the constant volume explosion governing equations (Eqs. 98 and 108) to determine the evolution of the thermodynamic state and the induction time. Our algorithm returns three different interpretations of the induction time, each dependent on the maximum temperature gradient. We looks for the time when the temperature gradient is maximum, the time when the temperature gradient has reached 90% of its maximum, and the time when the temperature gradient has reached 10% of its maximum.

6.3.1 Initial Conditions

The initial conditions for this model consist of a mixture of reactants at high temperature and pressure. The user can either specify the initial pressure and temperature desired or use the frozen post-shock

state calculator (Browne et al., 2007). In both demos included with the toolbox, the initial conditions are determined by shocking a mixture at standard temperature and pressure. In these cases, the user must specify the pre-shock initial conditions and either the desired shock speed or the option to use the Chapman-Jouguet detonation speed for the given mixture.

6.3.2 Algorithm

1. Define Known quantities: Upstream State (P_1, T_1, $\overline{Y}_1$), $\overline{W}$, $\mathcal{R}$, error tolerances
2. Seek Unknown quantities: Evolution of thermodynamic properties and species ($P(t)$, $T(t)$, $\overline{Y}(t)$) and induction time
3. Specify the initial state. To elevate the temperature and pressure by shocking the initial mixture, call program `PostShock_fr` (Browne et al., 2007). Both demos below begin with a shocked mixture.
   - `cv_shk` option implements `PostShock_fr` and requires the user to specify the shock speed.
   - The `cv_CJ` option implements `PostShock_fr` and assumes that the shock speed will be the CJ speed.
4. Call a stiff ODE solver (`ode15s` in Matlab, `CVODE` in c++) to iteratively solve Eqs. 98 and 108 subject to the equation of state (Eq. 2).
5. Create an array of the temperature gradient according to Eq. 108.
6. Find the three interpretations of the induction time
   - Coordinate of maximum temperature gradient
   - Coordinate when temperature gradient reaches 10% of its maximum
   - Coordinate when temperature gradient reaches 90% of its maximum
7. Return three values of the induction time and arrays for $P(t)$, $T(t)$, and $\overline{Y}(t)$

Figure 16 shows the agreement of our new implementation with the legacy Fortran version which uses the CHEMKIN thermodynamic library.

6.4 Example

Here will illustrate the results for a constant volume explosion starting from the von Neumann point. The von Neumann state is the frozen post-shock state behind a shock traveling at the CJ detonation velocity for the given mixture. See the following examples:
Matlab: demo_cvCJ.m and demo_cvshk.m
Python: demo_cvCJ.py and demo_cvshk.py

- CV basic
- Discuss Westbrook and Urtiew

The spatial profiles for pressure, temperature, density, velocity, and species for a constant volume explosion in a stoichiometric mixture of hydrogen and air initially at the von Neumann point (state 2 in Fig. 3) is shown in Figs. 17 and 18. We used the Matlab demonstration demo_cvCJ.m to generate these results. We calculate the induction time as the time corresponding to the maximum temperature gradient. The temperature gradient profile for this case is superposed on the temperature profile and shown in Fig. 19.

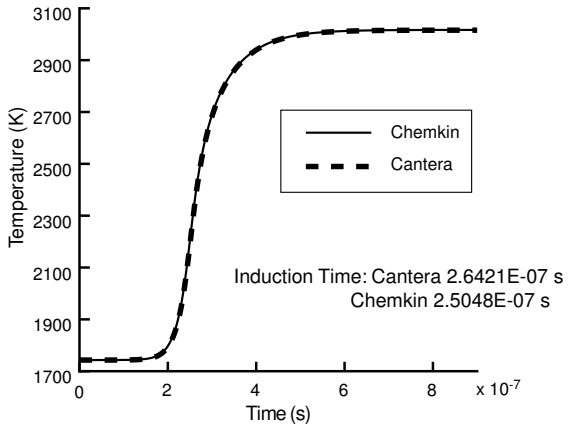

Figure 16: Control volume explosion simulated by PostShock_fr superimposed over control volume explosion simulated by Shepherd's CV program. The case is hydrogen air with an equivalence ratio of 0.5, an initial temperature of 300 K, an initial pressure of 1 atm, and a shock speed of 2000 m/s.

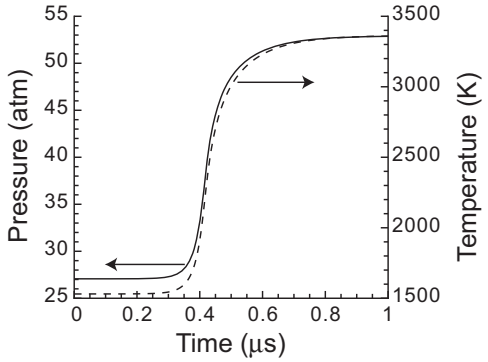

Figure 17: CV structure for a stoichiometric mixture of hydrogen-air initially at the von Neumann point. (a) temperature and pressure profiles, (b) density and velocity profiles

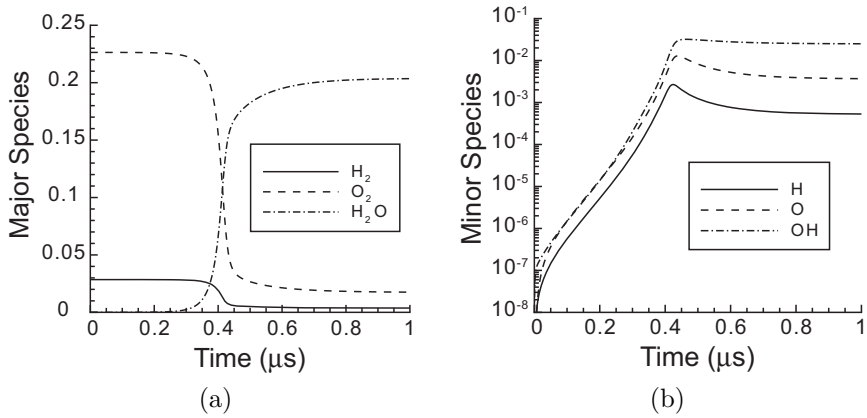

(a) (b)

Figure 18: CV structure for a stoichiometric mixture of hydrogen-air initially at the von Neumann point. (a) major species profiles, (b) minor species profiles

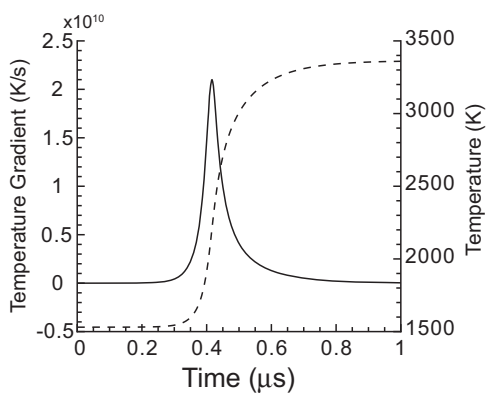

Figure 19: Temperature gradient and temperature CV structure for a stoichiometric mixture of hydrogen-air initially at the von Neumann point.

7 Constant Pressure Explosion Model

In this section, we will present the constant pressure explosion model which is a limiting case of the ZND model (see Section 4). We will first give a graphical interpretation and present the mathematical model. Then we will describe our algorithm, and finally give an example.

7.1 Physical Model

A second model which simplifies the ZND equations could monitor a small constant pressure packet of reacting gas. As described in Section 3, tracking the time evolution of a fluid packet is the Langragian description of the field. If the pressure is held constant, the Rayleigh line between the reactant and product Hugoniot curves is horizontal as shown in Figure 14 which implies infinitely slow combustion (w $\rightarrow \infty$).

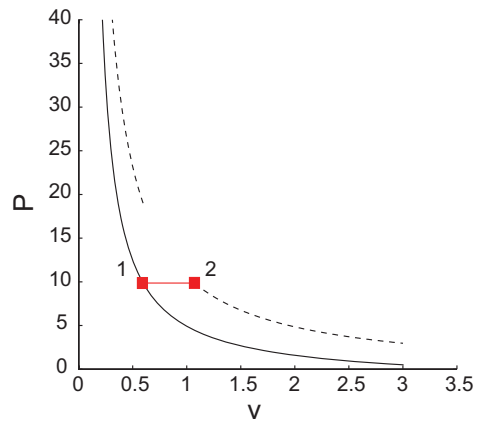

Figure 20: Path (red) between frozen Hugoniot (solid) and equilibrium Hugoniot (dashed) for a constant pressure explosion.

7.2 Mathematical Model

Like the ZND model (Section 4), the constant pressure explosion model can be expressed as a differential species conservation equation subject to algebraic physical constraints or as a purely differental system of equations.

7.2.1 Algebraic Differential System

The algebraic-differential system of equations corresponds to the Lagrangian conservation of species equation

$$\left.\frac{\mathrm{d}Y_i}{\mathrm{d}t}\right|_{X_p} = \dot{\Omega}_i, \tag{109}$$

where X_p is the particle path, and an algebraic constraint determined by the shock jump conditions (Eq. 15). The simplest way to specify this algebraic constraint is to examine the following form of the Hugoniot curve equation

$$\Delta h = \Delta P \frac{v_1 + v_2}{2}. \tag{110}$$

We see that if the pressure is constant then,

$$\Delta h = 0 \tag{111}$$

which is appropriate because in a constant pressure system, enthalpy is conserved. In the case of a perfect gas ($\gamma =$ constant) with a single progress variable, we can use

$$h(T) = \frac{\gamma}{\gamma - 1}\frac{P}{\rho} - \lambda q \tag{112}$$

to specify ρ in terms of species.

$$\rho = (\gamma - 1)\frac{h(T) + \lambda q}{P} \tag{113}$$

7.2.2 Differential System

The constant pressure explosion model is a Lagrangian model and therefore appears to be an unsteady zero-dimensional system of equations. For this model, we recall the definition of η (Eq. 70) and look at the limiting behavior of Eq. 75 as the velocity goes to zero. The limiting equations are

$$\left.\frac{\mathrm{d}\rho}{\mathrm{d}t}\right|_{X_p} = -\rho\dot{\sigma} \tag{114}$$

$$\left.\frac{\mathrm{d}\mathrm{w}}{\mathrm{d}t}\right|_{X_p} = 0 \tag{115}$$

$$\left.\frac{\mathrm{d}P}{\mathrm{d}t}\right|_{X_p} = 0 \tag{116}$$

$$\left.\frac{\mathrm{d}Y_i}{\mathrm{d}t}\right|_{X_p} = \dot{\Omega}_i. \tag{117}$$

We find that as expected the pressure remains constant and the density varies. We could also use the constant pressure limit of Eq. 27.

$$\left.\frac{\mathrm{d}h}{\mathrm{d}t}\right|_{X_p} = 0 \tag{118}$$

This corresponds more directly to Eq. 111. As in the constant volume model, we commonly compute the temperature as a function of time. The temperature equation can be derived from either energy equation (Eq. 116 or Eq. 118) or as the limit of the ZND temperature evolution equation (Eq. 82).

$$\left.\frac{\mathrm{d}T}{\mathrm{d}t}\right|_{X_p} = -\frac{1}{c_P}\sum_{i=1}^{N_Y} h_i\dot{\Omega}_i \tag{119}$$

A more detailed derivation of Eq. 119 is given in Appendix A

7.3 Numerical Method

7.4 Example

8 Applications

- Compare and contrast scales from ZND and CV

- Activation Energy
- τ, Δ vs $\phi, U/U_{CJ}, P_1$
- cell size correlations
- critical tube diameter

In this section we will present some useful applications for these programs. First in Section 8.1, we will compare the time scales computed with the ZND model and with those computed with the constant volume explosion model. As discussed in Section 6, the constant volume explosion model is often used as an approximation for the ZND model. We can also use these models to approximate the effective activation energy. A methodology for this is presented in Section 8.2. Section 8.3 uses these models to determine how the length and time scales vary with equivalence ratio, overdrive (U/U$_{CJ}$), and initial pressure. Finally, Section 8.4 gives some correlation expressions between the length and time scales and the dynamic detonation parameters (Lee, 1984).

8.1 Time Scale Comparison

8.2 Effective Activation Energy

8.3 Variance with Initial Conditions

8.4 Dynamic Detonation Parameters

9 Summary

ADD SECTION

References

J. B. Bdzil and D. S. Stewart. Modeling of two-dimensional detonations with detonation shock dynamics. *Phys. Fluids*, 1261, 1988. 31

S. Browne, J. Ziegler, and J. E. Shepherd. Numerical solution methods for shock and detonation jump conditions. Technical Report FM2006.007, GALCIT, 2007. 2, 6, 10, 12, 18, 19, 21, 25, 26, 27, 35

W. Doering. On detonation processes in gases. *Ann. Phys.*, 43:421–436, 1943. 19

C. A. Eckett. *Numerical and analytical studies of the dynamics of gaseous detonations*. PhD thesis, California Institute of Technology, Pasadena, California, September 2000. 11

C. A. Eckett, J. J. Quirk, and J. E. Shepherd. The role of unsteadiness in direct initiation of gaseous detonations. *J. Fluid Mech.*, 421:147–183, 2000. 31

W. Fickett and W. Davis. *Detonation Theory and Experiment*. Dover Publications, INC., 1979. 14, 25

D. Goodwin. Cantera: object-oriented software for reacting flows. Technical report, California Institute of Technology, 2005. http://www.cantera.org. 9

B. F. Gray and C. H. Yang. On the unification of the thermal and chain theories of explosion limits. *J. Phys. Chem.*, 69(8):2747–2750, 1965. 11

R. J. Kee, F. M. Rupley, and J. A. Miller. The CHEMKIN thermodynamic data base. Technical Report SAND87-8215, Sandia National Laboratories, 1987. 9

R. Klein, J. C. Krok, and J. E. Shepherd. Curved quasi-steady detonations: asymptotic analysis and detailed chemical kinetics. Technical Report FM95-04, California Institute of Technology, 1995. 31

V. P. Korobeinikov, V. A. Levin, V. V. Markov, and G. G. Cher. Propagation of blast wave in combustible gas. *Astronautica Acta*, 17:529–537, 1972. 11

J. H. Lee. Dynamic parameters of gaseous detonations. *Ann. Rev. Fluid Mech.*, 16:311–336, 1984. 40

M. H. Lefebvre, E. S. Oran, and K Kailasanath. Computations of detonation structure: The influence of model parameters. Technical Report NRL Memorandum Report NRL/MR/4404-92-6961, Naval Research Laboratory, 1992. 12

U. Maas and S. B. Pope. Simplifying chemical kinetics: Intrinsic low-dimensional manifolds in composition space. *Combust. Flame*, 88:239–264, 1992. 11

E. S. Oran, J. P. Boris, T. Young, M. Flanigan, T. Burks, and M. Picone. Numerical simulations of detonations in hydrogen-air and methane-air mixtures. In *18th Symp. (Intl) on Combustion*, pages 1641–1649, 1981. 11

N. Peters. Systematic reduction of flame kinetics: Principles and details. *Prog. Astronaut. Aeronaut.*, 113:67–86, 1988. 11

N. N. Semenov. *Chemical Kinetics and Chain Reactions*. Clarendon Press, Oxford, 1935. 11

J. E. Shepherd. Chemical kinetics of hydrogen–air–diluent detonations. *Prog. Astronaut. Aeronaut.*, 106:263–293, 1986. 9

G. P. Smith, D. M. Golden, M. Frenklach, N. W. Moriarty, B. Eiteneer, M. Goldenberg, C. T. Bowman, R. K. Hanson, S. Song, W. C. Gardiner, V. V. Lissianski Jr., and Z. Qin. GRI-Mechanism 3.0. http://www.me.berkeley.edu/gri_mech, 1999. 8, 9, 11

A. S. Tomlin, T. Turanyi, and M. J. Pilling. Mathematical tools for the construction, investigation, and reduction of combustion mechanisms. In M. J. Pilling, editor, *Low-temperature combustion and autoignition*, pages 293–437. Elsevier, 1997. 11

B. Varatharajan and F. A. Williams. Chemical-kinetic descriptions of high-temperature ignition and detonation of acetylene-oxygen-diluent systems. *Combust. Flame*, 124(4):623–645, 2001. 11

B. Varatharajan, M. Petrova, F. A. Williams, and V. Tangirala. Two-step chemical-kinetic description for hydrocarbon-oxygen-diluent ignition and detonation applications. In *Proc. Combust. Inst.*, volume 30, pages 1869–1877, 2005. 11

J. von Neumann. Theory of detonation waves. In A. J. Taub, editor, *John von Neumann, Collected Works*. Macmillan, New York, 1942. 19, 25

Ia. B. Zel'dovich. On the theory of the propagation of detonation in gaseous systems. *Zh. Eksp. Teor. Fiz.*, 10:542–568, 1940. 19, 25

A Temperature Derivatives

In order to derive find expressions for the temperature evolution of each model, we start with the ideal gas P-ρ-T relation.

$$P = \rho R T \tag{A.1}$$

This leads to the following logarithmic derivation relationship.

$$\frac{\mathrm{d}P}{P} = \frac{\mathrm{d}\rho}{\rho} + \frac{\mathrm{d}R}{R} + \frac{\mathrm{d}T}{T} \tag{A.2}$$

Here R is the gas-specific gas constant,

$$R = \frac{\mathcal{R}}{\overline{W}} = \mathcal{R} \sum_{i=1}^{N_Y} \frac{Y_i}{W_i}. \tag{A.3}$$

The derivative of R is related to the evolution of the species in the following way

$$\frac{\mathrm{d}R}{R} = \frac{1}{R} \sum_{i=1}^{N_Y} \frac{\mathcal{R}}{\overline{W}} \frac{\overline{W}}{W_i} \mathrm{d}Y_i = \sum_{i=1}^{N_Y} \frac{\overline{W}}{W_i} \mathrm{d}Y_i \tag{A.4}$$

Now the temperature derivative in a steady flow is

$$\frac{\mathrm{d}T}{\mathrm{d}x} = T \left[\frac{1}{P} \frac{\mathrm{d}P}{\mathrm{d}x} - \frac{1}{\rho} \frac{\mathrm{d}\rho}{\mathrm{d}x} - \sum_{i=1}^{N_Y} \frac{\overline{W}}{W_i} \frac{\mathrm{d}Y_i}{\mathrm{d}x} \right], \tag{A.5}$$

and if we insert the thermicity equations (Eqs. 71-74),

$$\frac{\mathrm{d}T}{\mathrm{d}x} = T \left[-\frac{\rho \mathrm{w}}{P} \frac{\dot{\sigma}}{\eta} + \frac{1}{\mathrm{w}} \frac{\dot{\sigma}}{\eta} - \sum_{i=1}^{N_Y} \frac{\overline{W}}{W_i} \frac{\dot{\Omega}_i}{\mathrm{w}} \right]. \tag{A.6}$$

By grouping terms and recalling the definition of the frozen sound speed $a_f^2 = \gamma P / \rho$, the temperature equation becomes

$$\frac{\mathrm{d}T}{\mathrm{d}x} = \frac{T}{\mathrm{w}} \left[\left(1 - \frac{\gamma \mathrm{w}^2}{a_f^2} \right) \frac{\dot{\sigma}}{\eta} - \sum_{i=1}^{N_Y} \frac{\overline{W}}{W_i} \dot{\Omega}_i \right]. \tag{A.7}$$

Finally, the ZND temperature equation is

$$\frac{\mathrm{d}T}{\mathrm{d}x} = \frac{T}{\mathrm{w}} \left[\left(1 - \gamma M^2 \right) \frac{\dot{\sigma}}{\eta} - \sum_{i=1}^{N_Y} \frac{\overline{W}}{W_i} \dot{\Omega}_i \right] \tag{A.8}$$

or

$$\left. \frac{\mathrm{d}T}{\mathrm{d}x} \right|_{X_p} = \mathrm{w} \frac{\mathrm{d}T}{\mathrm{d}x} = T \left[\left(1 - \gamma M^2 \right) \frac{\dot{\sigma}}{\eta} - \sum_{i=1}^{N_Y} \frac{\overline{W}}{W_i} \dot{\Omega}_i \right]. \tag{A.9}$$

A.1 Limiting Behavior

The constant volume explosion is the limit of the ZND equations as velocity goes to infinity $\mathrm{w} \to \infty$. The velocity only appears in the first term and its limit is

$$T\left(1-\gamma\tfrac{\mathrm{w}^2}{a_f^2}\right)\frac{\dot{\sigma}}{\left(1-\frac{\mathrm{w}^2}{a_f^2}\right)} \to T\gamma\dot{\sigma}. \tag{A.10}$$

Now we can rearrange the terms as follows to find the correct expression for the constant volume model.

$$\left.\frac{\mathrm{d}T}{\mathrm{d}x}\right|_{X_p} = T\left[\gamma\sum_{i=1}^{N_Y}\left(\frac{\overline{W}}{W_i}-\frac{h_i}{c_PT}\right)\dot{\Omega}_i-\sum_{i=1}^{N_Y}\frac{\overline{W}}{W_i}\dot{\Omega}_i\right] \tag{A.11}$$

$$= T\sum_{i=1}^{N_Y}\left[(\gamma-1)\frac{\overline{W}}{W_i}-\frac{\gamma}{c_P}\frac{h_i}{T}\right]\dot{\Omega}_i \tag{A.12}$$

$$= T\sum_{i=1}^{N_Y}\left[(\gamma-1)\frac{\overline{W}}{W_i}-\frac{e_i+R_iT}{c_vT}\right]\dot{\Omega}_i \tag{A.13}$$

$$= T\sum_{i=1}^{N_Y}\left[(\gamma-1)\frac{\overline{W}}{W_i}-\frac{e_i+R_iT}{c_vT}\right]\dot{\Omega}_i \tag{A.14}$$

$$= -\frac{1}{c_v}\sum_{i=1}^{N_Y}e_i\dot{\Omega}_i+T\sum_{i=1}^{N_Y}\left[(\gamma-1)\frac{\overline{W}}{W_i}-\frac{\mathcal{R}}{\overline{W}}\frac{\overline{W}}{W_i}\frac{\gamma-1}{R}\right]\dot{\Omega}_i \tag{A.15}$$

$$= -\frac{1}{c_v}\sum_{i=1}^{N_Y}e_i\dot{\Omega}_i+T\sum_{i=1}^{N_Y}\left[(\gamma-1)\frac{\overline{W}}{W_i}-(\gamma-1)\frac{\overline{W}}{W_i}\right]\dot{\Omega}_i \tag{A.16}$$

$$\left.\frac{\mathrm{d}T}{\mathrm{d}x}\right|_{X_p} = -\frac{1}{c_v}\sum_{i=1}^{N_Y}e_i\dot{\Omega}_i \tag{A.17}$$

On the other hand, the constant pressure model is the limit as the velocity goes to zero $\mathrm{w} \to 0$. Again, the velocity only appears in the first term and its limit is

$$T\left(1-\gamma\tfrac{\mathrm{w}^2}{a_f^2}\right)\frac{\dot{\sigma}}{\left(1-\frac{\mathrm{w}^2}{a_f^2}\right)} \to T\dot{\sigma}. \tag{A.18}$$

Now we can rearrange the terms as follows to find the correct expression for the constant volume model.

$$\left.\frac{\mathrm{d}T}{\mathrm{d}x}\right|_{X_p} = T\left[\sum_{i=1}^{N_Y}\left(\frac{\overline{W}}{W_i}-\frac{h_i}{c_PT}\right)\dot{\Omega}_i-\sum_{i=1}^{N_Y}\frac{\overline{W}}{W_i}\dot{\Omega}_i\right] \tag{A.19}$$

$$= T\sum_{i=1}^{N_Y}-\frac{h_i}{c_PT}\dot{\Omega}_i \tag{A.20}$$

$$\left.\frac{\mathrm{d}T}{\mathrm{d}x}\right|_{X_p} = -\frac{1}{c_P}\sum_{i=1}^{N_Y}h_i\dot{\Omega}_i \tag{A.21}$$

B Functions

This section is intended to be a quick reference for learning and usage. Please refer to the website for installation details.

Below we have provided a brief description of the functions in the Shock and Detonation Toolbox that numerically calculate shock jump conditions. For each function, we give links to the Matlab and Python implementations of these functions.

B.1 Constant Volume Explosion

- **cv_shk**
  Inputs Initial Conditions and Returns Plots of Constant Volume Explosion.
  Matlab Function - cv_shk.m
  Python Code - cv_shk (in CV.py)

- **cv_CJ**
  Inputs Initial Conditions and Returns Plots of Constant Volume Explosion for the CJ Case - Output File: "fname_Ucj.plt" compatible with Tecplot.
  Matlab Function - cv_CJ.m
  Python Code - cv_CJ (in CV.py)

- **explosion**
  Constant Volume Explosion, a "zero dimensional" implementation with no length scale.
  Matlab Function - explosion.m
  Python Code - explosion (in CV.py)

- **uvsys**
  ODE system for a constant-volume, adiabatic reactor. Evaluates the system of ordinary differential equations for an adiabatic, constant-volume, zero-dimensional reactor. It assumes that the 'gas' object represents a reacting ideal gas mixture. Based on `conuv.m` from the Cantera toolbox, this function contains the equations passed to `ode15s` for a constant volume explosion.
  Matlab Function - uvsys.m
  Python Code - N/A

B.2 ZND Detonation

B.2.1 Matlab Implementation

See the following Matlab examples:
demo_ZNDCJ.m and demo_ZNDshk.m

- **znd_shk**
  Inputs Initial Conditions and Returns Plots of ZND Detonation, assumming that the intial gas goes through a shock wave with a frozen (rather than chemically equilibrated) state. Output Files: "fname_U1_znd.plt" & "fname_U1_znd2.plt" compatible with Tecplot.
  Matlab Function - znd_shk.m

- **znd_CJ**
  Inputs Initial Conditions and Returns Plots of ZND Detonation for the CJ Case – Output Files: "fname_Ucj_znd.plt" & "fname_Ucj_znd2.plt" compatible with Tecplot.
  Matlab Function - znd_CJ.m

- **znd_detonation**
  ZND Model Detonation.
  Matlab Function - znd_detonation.m

- **ZNDReactor**
  Contains the set of ODE's to solve ZND Detonation Problem that are passed to `ode15s` for a ZND detonation.
  Matlab Function - ZNDReactor.m

B.2.2 Python/C++ Implementation

Cantera includes a python wrapper for the constant volume explosion model governing equations, but does not provide a wrapper for the ZND equations. We included a wrapper with the python version of the Shock and Detonation toolbox. In order to use this feature, the user must first compile the C++ program ZND. Instructions for doing this can be found on the C++ ZND Program website. Once this program is compiled, the user can run ZND simulations directly with an input file.

If the user would rather use python to create the appropriate input file and/or run the C++ program in a loop, they can use our wrapper. Details for using the wrapper are given on the Python Wrapper website.